

## Histological Study on Possible Therapeutic Effect of BM-MSCs on Healing of Lung Fibrosis Induced by CCl<sub>4</sub> with Reference to Macrophage Plasticity

Ghada Galal Hamam\*, Mona H Raafat and Hany KK Mostafa

Histology and Cell Biology Department, Faculty of Medicine, Ain Shams University, Cairo, Egypt

\*Corresponding author: Hamam GG, Histology and Cell Biology, Faculty of Medicine, Ain Shams University, Cairo, Egypt, Tel: 00201120388467; E-mail: ghada.hamam@yahoo.com

Received date: March 05, 2019; Accepted date: March 19, 2019; Published date: March 25, 2019

Copyright: © 2019 Hamam GG, et al. This is an open-access article distributed under the terms of the Creative Commons Attribution License, which permits unrestricted use, distribution, and reproduction in any medium, provided the original author and source are credited.

### Abstract

**Background:** Lungs are susceptible to several types of toxins. Macrophages may play role in lung fibrosis. Mesenchymal stem cells (MSCs) have several valuable functions that make them a promising therapeutic option in the field of regenerative medicine.

**Objectives:** Investigate possible therapeutic effects of bone marrow (BM)-MSCs on lung injury induced by carbon tetrachloride (CCl<sub>4</sub>) in adult rats with reference to role of macrophages plasticity.

**Material and methods:** Forty-five adult male albino Wistar rats were divided into four groups. Group I (control). Group II (CCl<sub>4</sub>): rats received intraperitoneal injection of CCl<sub>4</sub> [0.1 ml/100gm body weight] twice weekly for two weeks. Group III (BM-MSCs treated) received single injection of BM-MSCs after last injection of CCl<sub>4</sub> and were left for further two weeks. Group IV (recovery): were left for two weeks after last injection of CCl<sub>4</sub>. At the end of experiment, all rats were sacrificed. Lung specimens were processed and subjected to H&E, Mallory's trichrome, CD68, toluidine blue, transmission electron microscope and histomorphometric and statistical studies.

**Results:** CCl<sub>4</sub> and recovery groups showed thickening of interalveolar septa with mononuclear cellular infiltration, dissolved lamellar bodies in pneumocytes type-II and appearance of foamy macrophages. Significant increase in mean area percentage of collagen fibers, and mean number of CD68 macrophages were also noticed. BM-MSCs improved these histological changes with a significant increase number in pneumocyte type-II.

**Conclusions:** CCl<sub>4</sub> caused lung injury that was associated with inflammation, increased number of macrophages, and collagen fiber deposition. Treatment with BM-MSCs alleviates these changes and could be used in regenerative medicine.

**Keywords:** Lung; Stem cells; Histology; Macrophage; Electron microscope; CD68

### Introduction

The respiratory tract is a major target of oxidative damage caused by both endogenous and exogenous processes. The reactive species produced by phagocytes are the major cause of tissue damage associated with chronic inflammatory lung disease [1]. Carbon tetrachloride (CCl<sub>4</sub>) intoxication in animals is an experimental model that mimics oxidative stress in many pathophysiological situations [2,3]. Common diseases in the lung as asthma, chronic obstructive pulmonary disease and cystic fibrosis had been demonstrated to share similar pathogenesis with CCl<sub>4</sub> [3]. Pulmonary fibrosis is a severe and crippling disease with a poor prognosis [4] and it is the end stage for a wide range of lung inflammatory conditions [5].

Macrophages are present in virtually all the tissues of the body and play crucial roles in both acute and chronic pulmonary pathologies including cytotoxicity and fibrosis. Macrophages can be classified as M<sub>1</sub> or M<sub>2</sub> subtypes. They acquire their functional phenotype dependent on the inflammatory signals they encounter in tissue

microenvironment [6]. It was reported that fibrosis induced by bleomycin, silica dust, or thoracic radiation promotes early and sustained accumulation of lipid laden alveolar macrophages "foam cells" in the lung. Strategies aimed at blocking foam cell formation might be effective for treating fibrotic lung disorders [7].

Many lung diseases remain incurable and have substantial morbidity and mortality, although symptomatic care for these conditions has improved, but lung transplantation remains the only option for many patients. Furthermore, lung transplantation is associated with lifelong immunosuppression, and five years mortality of approximately 50%. New options are thus needed [8].

Mesenchymal stem cells (MSCs) hold great promise in disease treatment, especially in the fields of regenerative medicine, including inflammatory lung diseases [9]. During the past few years, numerous reports have shown that bone marrow (BM) derived MSCs and progenitor cells can give rise to differentiated cells of multiple non-hematopoietic organs including the lung [10]. Based on this, BM-MSCs are being exploited in the clinic for their therapeutic potential in chronic lung diseases, as chronic obstructive lung disease, pulmonary fibrosis, and pulmonary hypertension. MSCs have long been regarded

as ideal candidates for cell-based therapy of lung diseases because of their trans-differentiation potential, immunomodulatory properties (i.e., inhibition of lymphocyte proliferation) and possible enrolment in tissue repair [11].

## Aim of the Study

This study was designed to investigate the possible therapeutic effects of BM-MSCs on lung injury induced by CCL<sub>4</sub> in adult male albino rats with special reference to role of macrophage plasticity.

## Materials and Methods

### Animals

Forty-five adult male albino Wistar rats weighing 200-250 grams were purchased from Animal Research Center of Faculty of Medicine Ain Shams University. Their ages ranged from 3-4 months. Rats were housed in clean wire mesh cages under proper conditions of light/dark cycles, temperature and humidity. They were fed standard rat diet and water ad-libitum. The whole experiment was carried out in the Animal Research Center, Faculty of Medicine, Ain Shams University. Animal procedures were carried out according to the guideline of animal care and the scientific research ethical committee of the Faculty of Medicine, Ain Shams University.

### Preparation of CCL<sub>4</sub> solution

CCL<sub>4</sub> of 100% concentration (Sigma, St Louis, USA) and extra-virgin olive oil (Saporito Foods Inc., Markham, Ontario, Canada) were obtained from Algomhoria Company, Cairo, Egypt. CCL<sub>4</sub> was diluted in equal volume of extra-virgin olive oil (1:1) and was prepared freshly at time of use. It was given to rats (0.1 ml/100gm body weight) twice weekly by intraperitoneal injection (IP) [12].

### Culture, characterization and labelling of BM-MSCs

Rat BM derived -PKH26 labeled MSCs were purchased from Biochemistry Department, Faculty of Medicine, Cairo University in the form of vials [13]. Each vial contained 2.5x10<sup>6</sup> BM-MSCs suspended in 0.5ml phosphate buffer saline (PBS). The vials were maintained in ice box till injection. MSCs were harvested during the second passage and were labeled with PKH26 fluorescent dye. PKH26 is physiologically stable and shows little to no toxic side-effects on cell systems. It is a lipophilic dye that binds irreversibly to cell membranes and it is used to recognize transplanted stem cells in the host tissue by fluorescence microscopy. Labeled cells retain both biological and proliferating activity, and are ideal for in vitro cell labeling, in vitro proliferation studies and long-term in vivo cell tracking [14].

### Experimental protocol

Animals were kept for one week before the beginning of the experiment for acclimatization, and then they were randomly divided into four groups.

Group I (control group): included fifteen rats which were subdivided into three subgroups five rats each.

- Subgroup Ia: negative control group.

- Subgroup Ib: were given 0.1 ml/100 g body weight of extra-virgin olive oil by IP injection twice weekly for two weeks then that they were sacrificed.
- Subgroup Ic: were given extra-virgin olive oil as subgroup Ib for two weeks. Then rats received single injection of 0.5 ml PBS (Lonza, Basel, Switzerland) via tail vein. Rats were sacrificed after further two weeks (i.e., Four weeks from beginning of experiment).

Group II (CCL<sub>4</sub> group): included ten rats which were given CCL<sub>4</sub> twice weekly, for two weeks then they were sacrificed.

Group III (BM-MSCs treated group): included ten rats that were given CCL<sub>4</sub> as group II for two weeks. Then they were given a single injection of 2.5x10<sup>6</sup> fluorescent labeled BM-MSCs in 0.5 ml of PBS via tail vein [15]. Rats were sacrificed after further two weeks (ie. Four weeks from beginning of experiment).

Group IV (Recovery): included ten rats which were given CCL<sub>4</sub> as group II, then they were left without treatment for further two weeks, then they were sacrificed (ie. Four weeks from beginning of experiment).

### Sample Collection

At the end of the experiment, rats were anesthetized by intraperitoneal injections of ketamine-xylazine mixture at a dose of 100 mg/kg body weight for ketamine (ketalar 50 mg/ml; Pfizer, New York, USA) and xylazine 10 mg/kg body weight (Xylaject 20 mg/ml; Adwia, Egypt) [16], and then they were sacrificed by cervical dislocation. Thoracotomy incision was done and both lungs from each rat from different groups were carefully incised and removed from the thoracic cavity to be subjected to different histological preparations.

### Preparation of paraffin sections

The upper lobe of right lung was taken and fixed immediately in 10% formol saline solution and were then processed to obtain paraffin sections of 5µm thickness. Sections were subjected to H&E and Mallory's trichrome stain [17]. Other sections were cut on positively charged slides and were stained with avidin-biotin peroxidase technique for CD68 to detect (alveolar macrophage) at a dilution of (1:200). Sections were counter stained with Hematoxylin. Positive controls using liver tissue (for Kupffer cells) were processed according to the same protocol. Negative controls were processed according to the same protocol, except for the use of the primary antibody [17]. Antibodies against CD68 were purchased from (Cell Marque, Rocklin, CA, USA). Sections were examined and photographed with Olympus BX 40 light microscope (Olympus, Hamburg, Germany) connected to a camera Canon power shot A640 digital camera (Canon Inc., Tokyo, Japan) at Histology and Cell Biology Department Faculty of Medicine Ain Shams University.

### Preparation of transmission electron microscopic (TEM) study

The upper lobe of left lung was cut in small pieces about 1 mm<sup>3</sup> sizes and rapidly fixed in 2.5% glutaraldehyde for 24 hours. Specimens were processed for TEM study. Semithin sections (1 µm) were stained with 1% toluidine blue in borax [17] and were examined with light microscope. Ultrathin sections (50 nm) were examined and photographed with JEM 1200 EXII, TEM in Faculty of Science, Ain Shams University.

### Examination of PKH26 labelled MSCs

The unstained sections which were labeled by PKH26 were examined and photographed using Fluorescent Microscope (Olympus BX50F4, No. 7M03285, Tokyo, Japan) at Biochemistry Department, Faculty of Medicine, Cairo University.

### Morphometric and statistical analysis

Measures were obtained from all animals in each group. Five specimens from five different rats of each group were examined (n=5). For each specimen, five different captured non-overlapping fields were taken. Five different readings from every captured photo were counted and the mean was calculated for each specimen. Measurements were counted by an independent observer blinded to the specimens' details to perform an unbiased assessment. Samples were analyzed by using Leica DM2500 microscope with built in camera (Wetzlar, Germany). All images were digitally acquired using an image analyzer Leica Q win V.3 program (Wetzlar, Germany) installed on a computer in the Histology department faculty of Medicine Ain Shams University. The following parameters were measured:

- Thickness of inter-alveolar septum in Hx & E stained sections (X400).
- Number of pneumocytes type II in Toluidine blue stained sections (X400).
- Area% for collagen fibers content in Mallory Trichrome stained sections (X200).
- Number of CD68 positive cells (X400).

Data were collected, revised then subjected to statistical analysis using one-way ANOVA performed by SPSS.21 program (IBM Inc. Chicago, Illinois, USA). The significance of the data was determined by P value  $P > 0.05$  non-significant,  $P \leq 0.05$  significant.

## Results

### Mortality rate

One rat died in group II while three rats died from group IV during the experiment with mortality rate of 10% and 30% respectively. No further deaths were recorded in the other groups.

### Microscopic results

Examination using Fluorescent microscope in unstained sections of control group showed no red fluorescence (Figure 1A), while rats treated with BM-MSCs (group III), showed several red fluorescence of PKH26 labeled MSCs in the interalveolar septa (Figure 1B).

Examination of H&E stained sections of control group (subgroups Ia, Ib and Ic) showed similar findings. Lungs were formed of alveoli, alveolar sacs, alveolar ducts, respiratory bronchioles and bronchi. The wall of bronchioles was seen formed of three layers. The mucosa was formed of simple cuboidal epithelium and occasional club cells (formerly known as Clara cells) with underlying thin layer of lamina propria. Mucosa was followed by a layer of smooth muscle cells and adventitia. Alveoli were separated by thin interalveolar septa. They were lined by type-I pneumocytes with flat nuclei and cuboidal type-II pneumocytes with rounded nuclei (Figures 1C and 1D). In CCl<sub>4</sub> group, mononuclear cellular infiltration was frequently seen in the inter-alveolar septa and surrounding blood vessels. Most interalveolar septa were thickened with narrowing of most alveoli and compensatory

dilatation in others. Bronchioles were seen with detached epithelium, distorted smooth muscle layer and heavy mononuclear cellular infiltration in the adventitia. Most blood vessels were seen with thickened wall, disrupted endothelial lining, vacuolated smooth muscles in tunica media and acidophilic material in their lumen (Figures 1E and 1F).

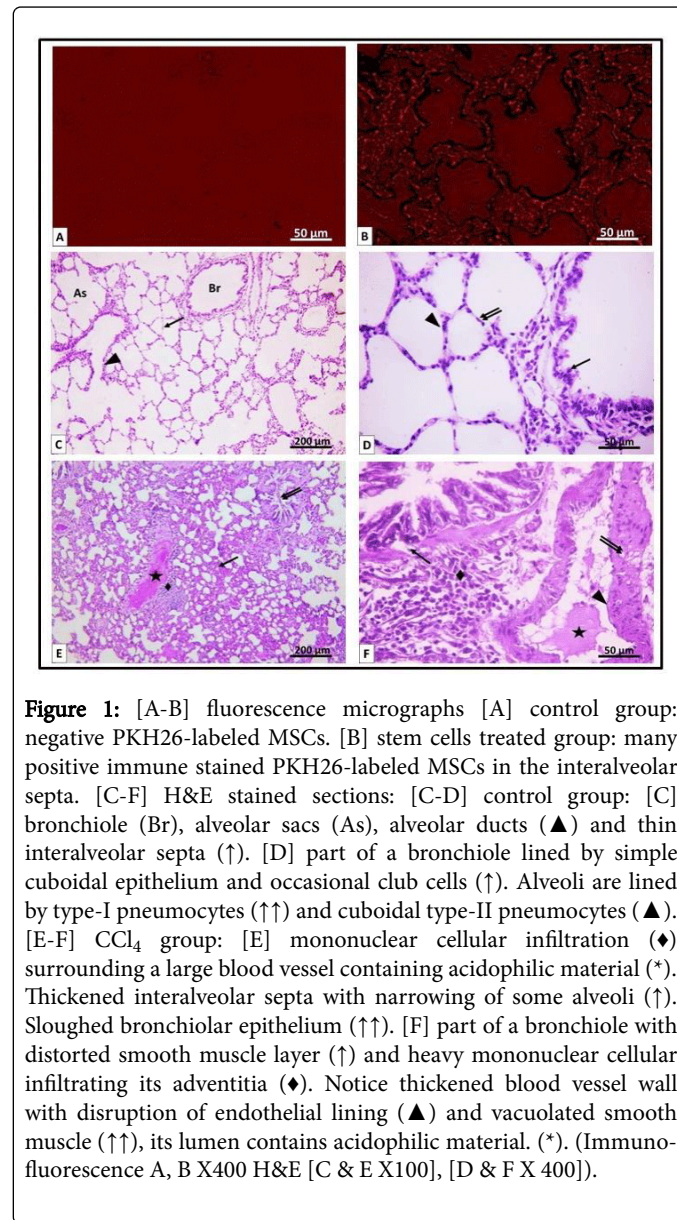


**Figure 1:** [A-B] fluorescence micrographs [A] control group: negative PKH26-labeled MSCs. [B] stem cells treated group: many positive immune stained PKH26-labeled MSCs in the interalveolar septa. [C-F] H&E stained sections: [C-D] control group: [C] bronchiole (Br), alveolar sacs (As), alveolar ducts (▲) and thin interalveolar septa (↑). [D] part of a bronchiole lined by simple cuboidal epithelium and occasional club cells (↑). Alveoli are lined by type-I pneumocytes (↑↑) and cuboidal type-II pneumocytes (▲). [E-F] CCl<sub>4</sub> group: [E] mononuclear cellular infiltration (◆) surrounding a large blood vessel containing acidophilic material (\*). Thickened interalveolar septa with narrowing of some alveoli (↑). Sloughed bronchiolar epithelium (↑↑). [F] part of a bronchiole with distorted smooth muscle layer (↑) and heavy mononuclear cellular infiltrating its adventitia (◆). Notice thickened blood vessel wall with disruption of endothelial lining (▲) and vacuolated smooth muscle (↑↑), its lumen contains acidophilic material. (\*). (Immunofluorescence A, B X400 H&E [C & E X100], [D & F X 400]).

In stem cells treated group, patent alveoli were separated by relatively thin interalveolar septa compared to group II and IV. Bronchioles were lined with low columnar cells alternating with numerous dome shaped club cells. Mononuclear cellular infiltrations were occasionally seen (Figures 2A and 2B), whereas in recovery group, most blood vessels were seen dilated congested with acidophilic material in their lumen. Mononuclear cellular infiltration and extravasations of red blood cells were frequently seen in the interalveolar septa and in the lumen of some alveoli. Bronchioles were lined with low columnar cells alternating with many dome shaped club cells. Most bronchial lumens were full of exfoliated epithelium and red

blood cells. Disruption of the alveolar wall and extravasations of red blood cells were frequently noticed (Figures 2C and 2D).

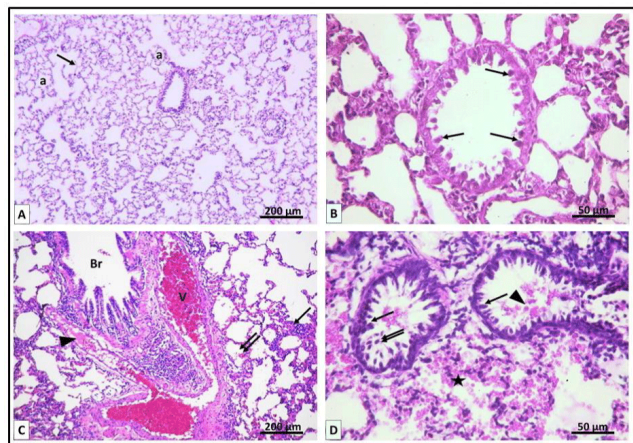


**Figure 2:** [A-B] stem cells treated group: [A] patent alveoli (a) are separated by thin interalveolar septa (↑). [B] Thin interalveolar septa. The bronchiole is lined with low columnar cells alternating with numerous dome shaped club cells (↑). [C-D] recovery group: [C] a bronchiole (Br) and dilated congested blood vessel (V) containing blood cells and acidophilic material (▲). Mononuclear cellular infiltration, extravasations of red blood cells in the interalveolar septa (↑) and in the lumen of some alveoli (↑↑). [D] bronchioles are lined with low columnar cells alternating with numerous dome shaped club cells (↑) their lumens are full of exfoliated spindle shaped cells (↑↑) and red blood cells (▲). Extravasations of red blood cells (★). (H&E [A & C X100], [B & D X 400]).

Examination of Mallory's trichrome stained sections of control group showed few collagen fibers in the interalveolar septa, surrounding bronchioles and blood vessels (Figure 3A). In CCl<sub>4</sub> group, massive deposition of collagen fibers was seen in the interalveolar septa and both in the lamina propria and adventitia of most bronchioles (Figure 3B). On the contrary in stem cells treated group, few collagen fibers were seen in the thin interalveolar septa and in the lamina propria and adventitia of some bronchioles (Figure 3C), while in recovery group, abundant collagen fibers were seen in the lung interstitium, around blood vessels and in the adventitia of most bronchioles (Figure 3D).

Immunohistochemical examination of CD68 sections of control group showed few positive CD68 interstitial macrophages in the interalveolar septa (Figure 4A), whereas, in CCl<sub>4</sub> group, numerous immune positive interstitial and alveolar macrophages were seen (Figure 4B). In stem cells treated group, few positive CD68 interstitial macrophages were noticed (Figure 4C), while in recovery group, multiple immune positive macrophages were seen in the interalveolar septa (Figure 4D).

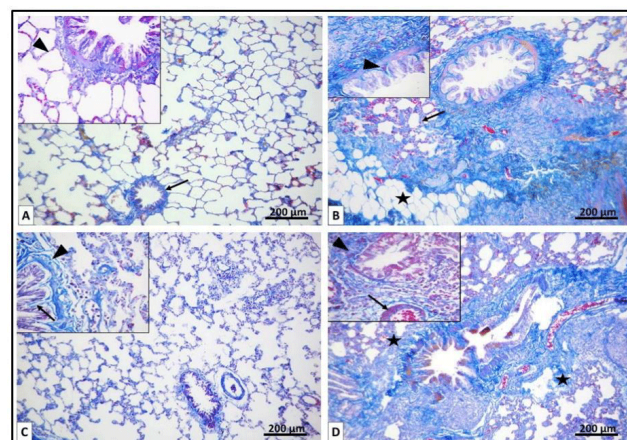


**Figure 3:** Mallory's trichrome stained sections. [A] control group: few collagen fibers (↑) surrounding bronchiole and a blood vessel. Inset: few collagen fibers in the interalveolar septa (▲). [B] CCl<sub>4</sub> group: massive collagen fibers deposition in the interalveolar septa (↑) and around bronchiole. Fat cells (\*) are seen in lung interstitium. Inset: collagen fibers in the lamina propria (▲) and adventitia of the bronchiole. [C] stem cells treated group: few collagen fibers in the thin interalveolar septa. Inset: few collagen fibers in the lamina propria (↑) and adventitia of the bronchiole (▲). [D] recovery group: abundant collagen fibers (\*) in the lung interstitium and around blood vessels. Inset: massive collagen fibers in the adventitia of the bronchiole (▲) and the blood vessels (↑). ([A, B, C, DX100], Insets X400).

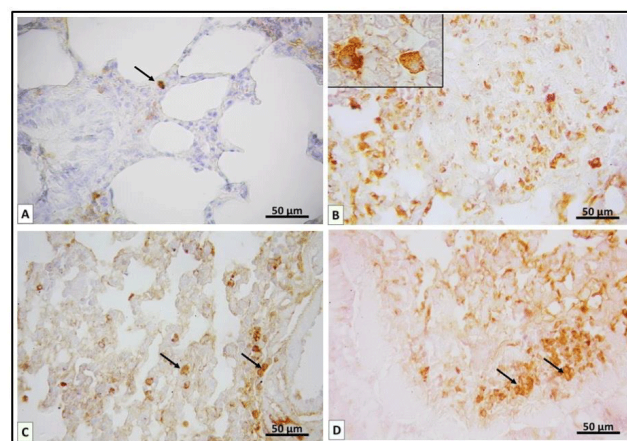


**Figure 4:** [A] control group: few positive CD68 macrophages in the interalveolar septa (↑). [B] CCl<sub>4</sub> group: numerous immune positive macrophages in the interalveolar septa. Inset: macrophages with eccentric nuclei. [C] stem cells treated group: few positive CD68 interstitial macrophages in the interalveolar septa (↑). [D] recovery group: multiple immune positive macrophages in the interalveolar septa (↑). (CD68 X 400, [inset of B X 1000]).

Examination of Toluidine blue stained semithin sections of control group showed thin interalveolar septa. Alveoli were lined by flat type-I

pneumocytes and dome shaped type-II pneumocytes with rounded nuclei and vacuolated cytoplasm (Figure 5A). However, in CCl<sub>4</sub> group, thickened interalveolar septa, dilated blood vessels, mononuclear cellular infiltration in the interalveolar septa and an increase number of pneumocytes type-II was frequently noticed (Figure 5B). In stem cells treated group, an increase in the number of type-II pneumocytes was noticed. Interalveolar septa were relatively thinner compared to CCl<sub>4</sub> group (Figure 5C). In recovery group, thick interalveolar septum and narrowing of most alveolar spaces, together with mononuclear inflammatory cellular infiltration and increased number and size of type-II pneumocytes were frequently noticed (Figure 5D).

Ultrastructure examination by Transmission electron microscope of control group showed type-I pneumocytes with thin attenuated cytoplasm and flattened nuclei. Blood capillary in the interalveolar septa were lined with flattened endothelial cells (Figure 6A). Dome shaped type-II pneumocytes with large euchromatic nuclei and numerous lamellar bodies were seen (Figure 6B). In CCl<sub>4</sub> group, most type-II pneumocytes were seen with irregular small electron-dense nuclei and contained variable sized empty lamellar bodies. Foamy macrophages, fibroblasts and nearby collagen fibrils were frequently seen (Figures 6C and 6D). Macrophages were frequently seen in lung interstitium and in alveolar lumen. They appeared foamy with large eccentric euchromatic nuclei and many electron dense endocytic vesicles (Figures 6E and 6F).

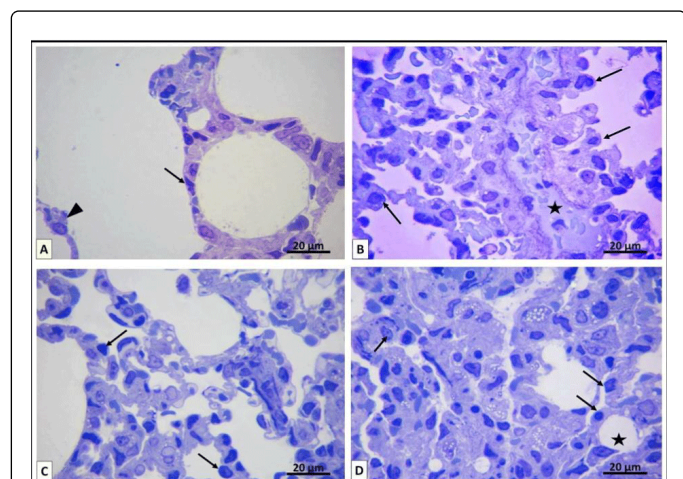


**Figure 5:** Semithin sections. [A] control group: thin interalveolar septa. Alveoli are lined by flat type-I pneumocytes (↑) and few dome shaped type-II pneumocytes (▲) with rounded nuclei and vacuolated cytoplasm. [B] CCl<sub>4</sub> group: thickened interalveolar septa and a dilated blood vessel (\*). Mononuclear cellular infiltrating the interalveolar septa an apparent increase number of pneumocytes type-II (↑). [C] stem cells treated group: increase number of type-II pneumocytes (↑). Notice the interalveolar septa are relatively thin compared to CCl<sub>4</sub> group. [D] recovery group: thick interalveolar septum and narrowing of most alveolar spaces (\*), together with mononuclear inflammatory cell infiltration. Notice increase number and size of type-II pneumocytes (↑). (Toluidine blue X1000).

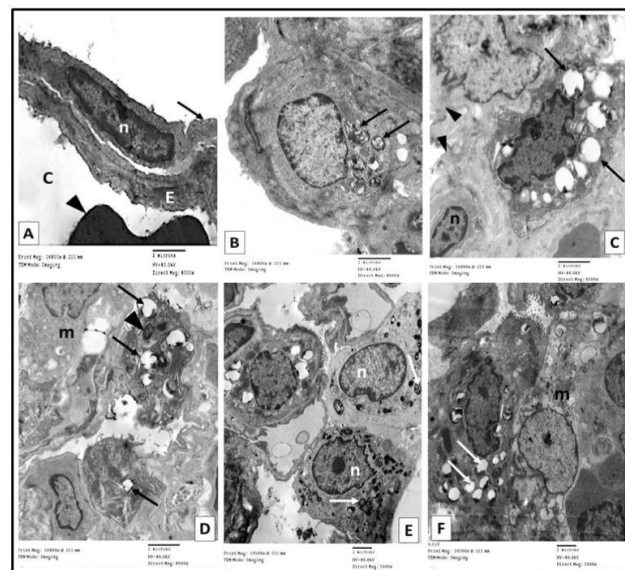


**Figure 6:** Electron micrographs [A-B] control group: [A] type-I pneumocyte with thin attenuated cytoplasm (↑) and flattened nucleus (n). Blood capillary (C) in the interalveolar septum lined with endothelial cell (E) and containing red blood cells (▲). [B] dome shaped type-II pneumocyte with large euchromatic nucleus and lamellar bodies (↑). [C-F] CCl<sub>4</sub> group: [C] type-II pneumocyte with irregular nucleus and variable size empty lamellar bodies (↑). Fibroblast with euchromatic nucleus (n) and nearby collagen fibrils (▲). [D] type-II pneumocytes with small electron-dense nucleus (▲) and partially dissolved dilated lamellar bodies (↑). Foamy macrophage (m) is also seen [E] macrophages with a large eccentric euchromatic nuclei (n) and many electron dense endocytic vesicles (↑). [F] foamy macrophage (m) and pneumocyte type-II with empty lamellar bodies (↑). (TEM [A, B, C & D X 8000], [E & F X 5000]).

In stem cells treated group, electron dense endocytic vesicles were also seen (Figure 7B). In recovery group, few of variable size depleted lamellar bodies. Thick inter alveolar septa, contained neutrophils with segmented nuclei (Figure 7C). Eosinophils with their bilobed nuclei and characteristic oval shaped granules were observed. Plasma cells were seen with euchromatic eccentric nuclei and dilated cisternae of rough endoplasmic reticulum. Large cells with large euchromatic nuclei and prominent nucleoli (Figure 7D). Foamy macrophages were frequently seen (Figure 7E). Fibroblasts with nearby collagen fibrils were also noticed (Figure 7F).

### Statistical results

The mean thickness of inter-alveolar septa in CCl<sub>4</sub> group showed a significant increase compared to all groups. Treatment with BM-MSCs showed a significant increase compared to control group and a significant decrease compared to CCl<sub>4</sub> and recovery groups.

The mean number of pneumocytes type-II in CCl<sub>4</sub> group showed significant increase compared to control and recovery groups, and a significant decrease compared to BM-MSCs treated group. BM-MSCs treated group showed a significant increase compared to all groups,

and recovery group showed a significant increase compared to control group.

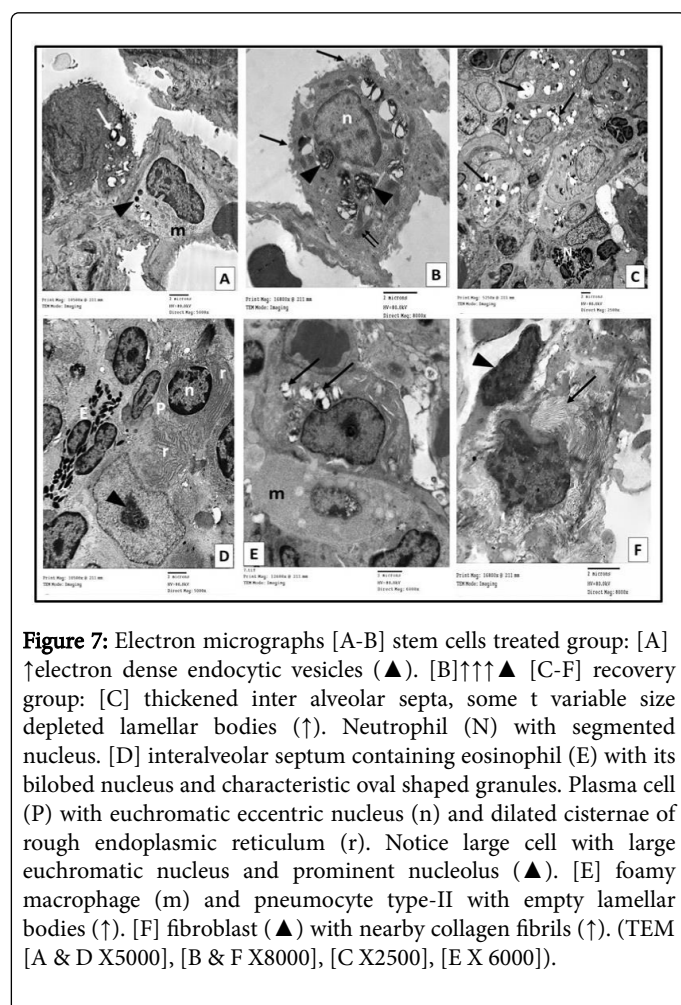
The mean area percentage of collagen fibers in CCl<sub>4</sub> and recovery groups showed a significant increase compared to control and stem cell treated groups. BM-MSCs treated group showed a significant increase compared to control group.

The mean number of CD68 positive macrophages in CCl<sub>4</sub> group showed a significant increase compared to control and stem cells treated groups, and a significant decrease compared to recovery group. Stem cells treated group showed a significant increase compared to control group and a significant decrease compared to CCl<sub>4</sub> and recovery groups. Recovery group showed a significant increase compared to all groups.

Group	Thickness of inter-alveolar septa (μm)	Number of pneumocytes type-II	Area % of Collagen fibers	Number of CD68 positive cells
Control group	3.36±0.13	4.4±0.33	5.81±0.34	1.8±0.24
CCl <sub>4</sub> group	31.09±1.2*	14.5±0.88*	41.51±1.01▲	37.4±1.57*
Stem Cells treated group	8.38±0.42*	25.2±0.9*	12.43±0.65*	9.3±0.33*
Recovery group	26.57±0.78*	12.3±0.51*	39.89±1.47▲	41.1±0.71*

\*Significant change compared to all groups  
▲Significant change compared to control and stem cell treated groups

**Table 1:** showing mean ± standard error of the thickness of inter-alveolar septa, number of pneumocytes type-II, area percentage of collagen fibers and number of CD68 positive cells and in different groups.



## Discussion

Pulmonary fibrosis is a progressive and severe disease [18] that may increase risk of pulmonary heart disease, seriously affecting the patients' health and quality of life [19]. There are two competing theories regarding the pathogenesis of lung fibrosis; one proposes that epithelial cell injury is the inciting event, and the other proposes that inflammation drives the development of the disease [7].

Many cases of lung inflammation and fibrosis are resistant to treatment, so the development of new treatments is required. Studies on MSCs have recently been actively performed in the field of regenerative medicine research [20]. Macrophages play key roles in fibrosis and inflammation. Pulmonary macrophages or their products are involved at each of the key stages of fibrotic process [21]. Macrophage directed therapy, is considered a novel therapeutic strategy for pulmonary fibrosis. This study was designed to study role of macrophage and BM-MSCs in lung fibrosis, as cellular transplantation or blockade of macrophages products, or combination of them, might prove a novel therapy.

In the current study, induction of pulmonary fibrosis was induced by CCl<sub>4</sub>. Pneumocyte type-II appeared with heterochromatic nuclei and vacuoles of depleted surfactant. Foamy macrophages were also frequently noticed inside alveoli and in lung interstitium. It was reported that the precise regulation of surfactant lipids requires a balance between synthesis and clearance. Lipid clearance is ordinarily mediated by pneumocyte type-II and, to a lesser extent, alveolar macrophages. It was also declared that type-II pneumocyte respond to injury by dumping surfactant lipids in the air spaces. In lung injury, the reuptake of surfactant lipid by type-II pneumocyte was also impaired. Lipid accumulation serves as an important stimulus for macrophage influx into the lung. Lipid-laden alveolar macrophages are also called "foam cells" [7].

Macrophages are classified as M<sub>1</sub> or M<sub>2</sub> subtypes depending on their functional phenotypes. The classically activated macrophages (i.e. M<sub>1</sub>), are characterized by their ability to induce inflammatory responses

[22] and production of high levels of pro-inflammatory cytokines. The alternatively activated, anti-inflammatory macrophages (M<sub>2</sub>) are characterized by their involvement in tissue remodeling, immune regulation and efficient phagocytic activity [23]. On the contrary it was reported that fibrotic insults upregulate lipid receptors resulting in change in macrophage gene expression from M<sub>1</sub> to M<sub>2</sub> [7]. In fibrotic lungs, macrophages are mainly M<sub>2</sub> macrophages. In vitro studies showed that recruited M<sub>2</sub> macrophages release high levels of Wnt7a, which activates the Wnt/ $\beta$ -catenin signaling pathway promoting differentiation of lung resident-MSCs into myofibroblast [6]. It was also reported that when macrophages are activated they release some inflammatory mediators, oxygen free radicals, and fibrogenic factors, as TGF- $\beta$ 1 [19]. Moreover, it was declared that macrophage depletion ameliorated fibrotic disease. Also, deletion of TGF- $\beta$  receptors in type-II pneumocytes and fibroblasts could protect against fibrosis [21]. Macrophages can also stimulate epithelial cells by releasing inflammatory cytokines as TNF- $\alpha$ , IL-1, IL-6 and IL-10. The activated epithelial cells can regulate local immunity through autocrine and paracrine signaling pathways [24]. This could explain the concomitant significant ( $p < 0.05$ ) increase in the mean number of macrophages and the mean area percentage of collagen fibers observed in the current study -in both CCl<sub>4</sub> and in recovery groups- compared to control and stem cells treated groups.

In CCl<sub>4</sub> and recovery groups of the current study, mononuclear cellular infiltration was noticed in interalveolar septa, around bronchioles and blood vessels. It was also reported that inflammatory responses are associated with the initial stage of pulmonary fibrosis [5], with influx of macrophages, neutrophils and lymphocytes [4]. This resulted in increased collagen gene expression and abnormal collagen deposition in the lungs [24].

Regarding mechanism of action of CCl<sub>4</sub>, it was reported that metabolic conversion of CCl<sub>4</sub> by cytochrome P-450 produces the reactive metabolite trichloromethyl radical ( $\bullet\text{CCl}_3$ ). As O<sub>2</sub> tension rises, a greater fraction of  $\bullet\text{CCl}_3$  reacts very rapidly with O<sub>2</sub> and more reactive free radicals, like trichloromethyl peroxide radical (CCl<sub>3</sub>OO $\bullet$ ) is generated from  $\bullet\text{CCl}_3$ . These free radicals initiate the peroxidation of membrane poly unsaturated fatty acids, causing cell necrosis, membrane damage and loss of antioxidant enzyme activity [2,25].

In the current study, congestion and thickening of the wall of blood vessels was noticed in CCl<sub>4</sub> group. This was explained by some authors who reported that CCl<sub>4</sub> induced thickness of vessel wall was due to increase pressure in intrapulmonary vessels. Previous studies reported that humoral factors derived from the splanchnic circulation, which would normally be metabolized in the liver, reach the pulmonary circulation due to portosystemic shunts and liver failure. These substances modify the endothelial cell function and promote vasoconstriction and thrombosis in pulmonary circulation [1]. Also activated macrophages release inflammatory cytokines as TNF- $\alpha$  and IL-1 [24], that stimulates endothelial cells to express adhesion molecules and chemokines which attract other white cells from the blood to the site of injury and stimulate proliferation of endothelial cells and fibroblasts [26].

Regarding the role of type-II alveolar epithelial cells in lung fibrosis, it was reported that they promote pulmonary fibrosis after acquiring the fibroblast phenotype through epithelial mesenchymal transition (EMT) [27]. EMT, is a process by which differentiated alveolar epithelial cells undergo a phenotypic conversion that gives rise to the matrix-producing fibroblasts and myofibroblasts [19,28]. EMT plays an important role in the initiation and progression of pulmonary

fibrosis in response to epithelial injury [19,27,28]. Evidence links injury/death of type-II alveolar epithelial cells to development of fibrosis. Possible mechanisms include either loss of anti-fibrotic functions supplied by healthy cells or an up-regulation of pro-fibrotic factors from the injured alveolar epithelial cells. Cellular apoptosis terminates with formation of vesicles termed apoptotic bodies. Apoptotic cells and bodies undergo phagocytosis in a process known as efferocytosis (or the phagocytic uptake of apoptotic cells) [29,30]. Efferocytosis prevents the dead cells from releasing pro-inflammatory molecules and antigens that have the potential to cause autoimmunity [30]. Alveolar macrophages ingest apoptotic type-II alveolar epithelial cells and this uptake induces a phenotypic shift that favors profibrotic gene expression and up-regulation of TGF- $\beta$  [31]. Recruited non-resident macrophages or other inflammatory cell types may also engulf apoptotic cells and contribute significantly to the fibrotic process [29,32]. It was also reported that alveolar injury activates alveolar epithelial cells to release profibrotic agents as matrix metalloproteinases and TGF- $\beta$  [33].

In the current study, rats left without treatment in recovery group, showed worsening of histological findings with significant increase in the mean area percentage of collagen fibers. Large cells containing large nuclei and prominent nucleoli were also frequently noticed in ultrathin sections. These cells could represent lung resident stem cell. This was explained by some authors who reported that lung resident MSCs are precursors of myofibroblasts and increase inflammatory responses that are associated with the development of pulmonary fibrosis [5,6]. It was added that lung resident MSCs can differentiate into several cells that may participate in lung repair or contribute to development of pulmonary diseases. TNF- $\alpha$  can induce EMT-MSCs to differentiate into myofibroblasts through activating NF- $\kappa$ B signaling [5].

In the current study, treatment with BM-MSCs resulted in improvement of histological findings. Thin septa with fewer mononuclear cellular infiltrations, and significant increase number of pneumocytes type-II were noticed. It was reported that administration of MSCs resulted in increased alveolar epithelial type-II cells, decrease collagen content in lung and reduced pulmonary TGF- $\beta$  levels. BM-MSCs also activate lung resident stem cells [33] and have potential antifibrotic properties [9,18,28,33,34]. This might explain the significant decrease in the mean area percentage of collagen fibers in stem cell treated group that was observed in the present study.

In the current study, a significant increase in the number of type-II pneumocytes was noticed in stem cell treated group. This could be explained by some authors who reported that BM-MSCs decrease apoptosis of type-II pneumocyte [18,33]. Others reported that type-II alveolar cells are progenitor cells for type-I alveolar cells, and after lung injury, they proliferate and restore both types of alveolar cells. Hyperplasia of type II alveolar cells is an important marker of alveolar injury and repair of alveoli [18,35]. An apparent increase number of club cells were also noticed in stem cell treated group in the current study. This might be a compensatory mechanism to replace damaged cells as it was reported that although club cells are functionally differentiated cells, but they retain progenitor cell activity. They can self-renew and generate ciliated cells during epithelial homeostasis and in response to lung damage. Using cell lineage tracing methods in mice showed that club cells can also give rise to alveolar epithelium type-II and type-I during repair processes of the alveolar epithelium damage [18].

BM-MSCs exert pleiotropic effects in lung injury. They have anti-apoptosis and anti-inflammatory actions, they modulate the immune response [9,18,20,33,34]. MSCs also reduce oxidative stress [18,33,34], and reduce the injury of alveolar epithelial cells in vivo [28]. They preserve pulmonary endothelial cell integrity by preserving adherent junctions and tight junctions. BM-MSCs protect lung tissue from injury by blocking TNF- and IL-1, the two fundamental proinflammatory cytokines in the lung [26]. The inhibition of EMT and protection of epithelial cells from damage may be an important cause of alleviating fibrotic progress by BM-MSCs [28].

In the current study, sections of CD68 revealed a significant decrease in the number of macrophages in stem cell treated group. It was reported that MSCs induced apoptosis of activated macrophages [20] by suppressing the Wnt/ $\beta$ -catenin signaling pathway that was known to be abnormally activated in lung fibrosis [28,36]. MSCs can interact with alveolar macrophages via cell-to-cell contact and promote their reprogramming [9].

## Conclusion and Recommendation

CCL<sub>4</sub> caused lung injury that was associated with inflammation, increased number of macrophages, and collagen fiber deposition. Treatments with BM-MSCs alleviate these changes and could be used in regenerative medicine. It is recommended to study the long-term safety of transplanted BM-MSCs on lung repair in different models of lung injury.

## References

1. Ferrari RS, da Rosa DP, Forgiarini LF, Bona S, Dias AS, et al. (2012) Oxidative Stress and Pulmonary Changes in Experimental Liver Cirrhosis. *Oxid Med Cell Longevity*.
2. Ganie AS, Haq E, Hamid A, Qurishi Y, Mahmood Z, et al. (2011) Carbon tetrachloride induced kidney and lung tissue damages and antioxidant activities of the aqueous rhizome extract of *Podophyllum hexandrum*. *BMC Complement Altern Med* 11: 17.
3. Ibrahim AE, Al-Shathly MR (2014) Evaluation of the anti-proliferative and immunomodulatory effect of sallyl cysteine on pulmonary fibrosis induced-rats. *Int J Plant Anim Environ Sci*.
4. Robert S, Gicquel T, Victoni T, Valenc S, Barreto E, et al. (2016) Involvement of matrix metalloproteinases (MMPs) and inflammasome pathway in molecular mechanisms of fibrosis. *Biosci Rep* 36: e00360.
5. Hou J, Ma T, Cao H, Chen Y, Wang C, et al. (2018) TNF- $\alpha$ -induced NF- $\kappa$ B activation promotes myofibroblast differentiation of LR-MSCs and exacerbates bleomycin-induced pulmonary fibrosis. *J Cell Physiol* 233: 2409-2419.
6. Hou J, Shi J, Chen L, Lv Z, Chen X, et al. (2018) Macrophages promote myofibroblast differentiation of LR-MSCs and are associated with pulmonary fibrogenesis. *Cell Commun Signaling* 16: 89.
7. Romero F, Shah D, Duong M, Penn RB, Fessler MB, et al. (2015) A pneumocyte-macrophage paracrine lipid axis drives the lung toward fibrosis. *Am J Respir Cell Mol Biol* 53: 74-86.
8. Sueblinvong V, Weiss DJ (2010) Stem cells and cell therapy approaches in lung biology and diseases. *Transl Res* 156: 188-205.
9. Fujita Y, Kadota T, Araya J, Ochiya T, Kuwano K (2018) Clinical Application of Mesenchymal Stem Cell-Derived Extracellular Vesicle-Based Therapeutics for Inflammatory Lung Diseases. *J Clin Med* 7: 355.
10. Grove JE, Bruscia E, Krause DS (2004) Plasticity of bone marrow-derived stem cells. *Stem Cells* 22: 487-500.
11. Zulueta A, Colombob M, Pelia V, Fallenic M, Tomic D, et al. (2018) Lung mesenchymal stem cells-derived extracellular vesicles attenuate the inflammatory profile of Cystic Fibrosis epithelial cells. *Cell Signal* 51: 110-118.
12. Pääkkö P1, Anttila S, Sormunen R, Ala-Kokko L, Peura R, et al. (1996) Biochemical and morphological characterization of carbon tetrachloride-induced lung fibrosis in rats. *Arch Toxicol* 70: 540-552.
13. Rochefort GY, Vaudin P, Bonnet N, Pages JC, Domenech J, et al. (2005) Influence of hypoxia on the domiciliation of mesenchymal stem cells after infusion into rats: possibilities of targeting pulmonary artery remodeling via cells therapies? *Respir Res* 6: 125.
14. Haas SJ, Bauer P, Rolfs A, Wree A (2000) Immunocytochemical characterization of in vitro PKH26-labelled and intracerebrally transplanted neonatal cells. *Acta Histochem* 102: 273-280.
15. Huang K, Wu XM, Wang XY, Kang XW, Xiao JL, et al. (2012) The effect of marrow mesenchymal stem cell transplantation on pulmonary fibrosis in rats. *Zhonghua Jie He He Hu Xi Za Zhi* 35: 659-664.
16. Abd El Samad AA, Raafat MH, Shokry Y, Abu Zahra FA, Abdellah AM (2015) Histological study on the role of bone marrow-derived mesenchymal stem cells on the sciatic nerve and the gastrocnemius muscle in a model of sciatic nerve crush injury in albino rats. *Egyptian Journal of Histology* 38: 438-451.
17. Suvarna K, Layton C, Bancroft J (2013) Theory and practice of histological techniques (7th edn.). Churchill Livingstone, USA 203: 500.
18. Serrano-Mollar A (2018) Cell Therapy in Idiopathic Pulmonary Fibrosis. *Med Sci (Basel)* 6: 64.
19. Guoa J, Yangb Z, Jiab Q, Bob C, Shaob H, et al. (2019) Pirfenidone inhibits epithelial-mesenchymal transition and pulmonary fibrosis in the rat silicosis model. *Toxicology Letters* 300: 59-66.
20. Kotani T, Masutani R, Suzuka T, Oda K, Makino S, et al. (2017) Anti-inflammatory and anti-fibrotic effects of intravenous adipose derived stem cell transplantation in a mouse model of bleomycin induced interstitial pneumonia. *Scientific Reports*.
21. Byrne AJ, Maher TM, Lloyd CM (2016) Pulmonary Macrophages: A New Therapeutic Pathway in Fibrosing Lung Disease? *Trends Mol Med* 22: 303-316.
22. Martinez FO, Gordon S (2014) The M1 and M2 paradigm of macrophage activation: time for reassessment. *F1000Prime Rep* 6: 13.
23. Chen S, Cui G, Peng C, Lavin MF, Sun X, et al. (2018) Transplantation of adipose-derived mesenchymal stem cells attenuates pulmonary fibrosis of silicosis via anti-inflammatory and anti-apoptosis effects in rats. *Stem Cell Res Ther* 9: 110.
24. Ahmed B, Khan MR, Shah NA (2013) Amelioration of carbon tetrachloride induced pulmonary toxicity with oxalis corniculata. *Toxicol Ind Health* 31: 1243-1251.
25. Li M, Ikehara S (2013) Bone-marrow-derived mesenchymal stem cells for organ repair. *Stem Cells Int*.
26. Du J, Zhu Y, Meng X, Xie H, Wang J, et al. (2018) Atorvastatin attenuates paraquat poisoning-induced epithelial mesenchymal transition via downregulating hypoxia-inducible factor-1 alpha. *Life Sciences* 213: 126-133.
27. Zhang E, Yang Y, Chen S, Peng C, Lavin MF, et al. (2018) Bone marrow mesenchymal stromal cells attenuate silica-induced pulmonary fibrosis potentially by attenuating Wnt/ $\beta$ -catenin signaling in rats. *Stem Cell Res Ther* 9: 311.
28. Kim KK, Dotson MR, Agarwal M, Yang J, Bradley P, et al. (2018) Efferocytosis of apoptotic alveolar epithelial cells is sufficient to initiate lung fibrosis. *Cell Death Dis* 9: 1056.
29. Mc Cubbrey AL, Curtis JL (2013) Efferocytosis and lung disease. *Chest* 143: 1750-1757.
30. Elliott MR, Koster KM, Murphy PS (2017) Efferocytosis signaling in the regulation of macrophage inflammatory responses. *J Immunol* 198: 1387-1394.
31. Misharin, AV, Nebreda LM, Reyfman PA, Cuda CM et al. (2017) Monocyte-derived alveolar macrophages drive lung fibrosis and persist in the lung over the life span. *J Exp Med* 214: 2387-2404.
32. Tzouveleki A, Toonkel R, Karampitsakos T, Medapalli K, Ninou I, et al. (2018) Mesenchymal Stem Cells for the Treatment of Idiopathic Pulmonary Fibrosis. *Front Med* 5:142.

- 
33. Mohammadipoor A, Antebi B, Batchinsky AI, Cancio LC (2018) Therapeutic potential of products derived from mesenchymal stem/stromal cells in pulmonary disease. *Respir Res* 19: 218.
34. Ross MH, Pawlina W (2015) *Histology: A Text and Atlas with correlated cell and molecular biology* (7th edn.). Wolters Kluwer Philadelphia, New York.
35. Henderson WR, Chi EY, Ye X, Nguyen C, Tien YT, et al. (2010) Inhibition of Wnt/beta-catenin/CREB binding protein (CBP) signaling reverses pulmonary fibrosis. *Proc Natl Acad Sci U S A* 107: 14309-14314.